Metallization of cyanide-modified Pt(111) electrodes with copper

Escudero-Escribano, Maria; Wildi, Christopher; Mwanda, Jonathan Amolo; Cuesta Ciscar, Angel

Published in:
Journal of Solid State Electrochemistry

DOI:
10.1007/s10008-015-2968-7

Publication date:
2016

Document Version
Peer reviewed version

Metallization of cyanide-modified Pt(111) electrodes with copper[1]

María Escudero-Escribano[1], Christopher Wildi[2], Jonathan A. Mwanda[2], and Angel Cuesta[2,*]

[1]*Center for Individual Nanoparticle Functionality, Department of Physics, Technical University of Denmark, Building 312, DK-2800 Lyngby, Denmark*

[2]*Department of Chemistry, School of Natural and computing Sciences, University of Aberdeen, Aberdeen AB24 3UE, UK*

*Corresponding Author. E-mail: angel.cuestaciscar@abdn.ac.uk

Abstract: The reduction of Cu^{2+} ions irreversibly anchored on the surface of a cyanide-modified Pt(111) electrode via non-covalent or weakly covalent interactions with the N atom of adsorbed cyanide was studied using cyclic voltammetry (CV) and in-situ scanning tunneling microscopy (STM). Both CV and STM provide evidence that the reduction of irreversibly adsorbed Cu^{2+} to Cu in Cu^{2+}-free sulfuric acid solutions does not result in the stripping of the cyanide adlayer. This strongly suggests that the reduction process results in the metallization of the cyanide adlayer on Pt(111), yielding a platinum-cyanide-copper sandwich configuration. STM also shows that the Cu deposit consists of isolated bidimensional nanoislands, which slowly grow through an Ostwald ripening mechanism if the potential is kept negative of the reduction peak. Metallization is not possible in perchloric acid solutions, which implies that the specific adsorption of sulfate on the bidimensional Cu nanoislands plays an important role in stabilizing them. This was confirmed by the observation on the nanoislands, using in-situ STM, of the structure typical for adsorbed sulfate on the (111) faces of fcc.

Keywords: platinum; copper; cyanide; SAMs; metallization; electroreduction; STM

[1] Dedicated to Prof. Dr. José H. Zagal on the occasion of his 65th birthday in recognition of his outstanding contributions to interfacial electrochemistry.

Introduction

The use of molecules as components of electronic circuits is the ultimate limit in the device miniaturization process experienced during the last decades, mainly led by the need of the microelectronics, data storage and communication industries for ever smaller feature sizes. Transport of electrons across single molecule junctions has been the object of intensive research [1-11], but less attention has been devoted to the development of simple means to produce electrical contacts across small groups of molecules, which will most likely be required for future applications of molecular electronics [12,13]. One possibility of achieving the latter objective is to sandwich a small group of molecules between a metallic or semiconducting substrate and a metal (preferably bidimensional) nanoisland. Early attempts to deposit a metal layer on top of a self-assembled monolayer (SAM), either by deposition from the gas phase [14,15] or electrochemically [16-25] were unsuccessful, and resulted in the metal creeping underneath the SAM and depositing directly onto the substrate. However, in 2004 Kolb and co-workers demonstrated the electrochemical metallization of an organic SAM to be possible, by simply preadsorbing the target metal cation (M^{z+}) on the SAM, and then reducing it in a M^{z+}-free electrolyte [26-32]. This method of SAM metallization has been later used by other groups [33,34], although in these cases 3D metal nanoparticles, rather than 2D nanoislands like in the work of Kolb and co-workers, were deposited on the organic adlayer.

An interesting further development of the work described above would be the metallization of molecular adlayers with ordered arrays of nanoislands of the same size. In such an arrangement, the number of molecules sandwiched between the nanoisland and the substrate would be the same in all the cases (increasing the reproducibility of the electrical-transport properties of the junctions), and novel collective phenomena could arise. Achieving this goal will require a careful design of the molecular adlayer, so that the metal deposit can be forced to form and stay at specific sites. As a first step along this path, we have decided to study the metallization of cyanide-modified Pt(111) electrodes.

We have recently attempted to deposit copper on cyanide-modified Pt(111) electrodes from Cu^{2+}-containing sulfuric acid solutions, which resulted in the stripping of the cyanide adlayer and the deposition of Cu onto the Pt substrate [35]. We have also shown that Cu^{2+} [35], as well as alkali-metal cations [36], can be incorporated into the electrical double layer via non-covalent interactions with the nitrogen atom of cyanide-modified Pt(111) surfaces. In the case of Cu^{2+}, the interaction is irreversible, and the cation remains attached to the electrode surface even after emersion from the Cu^{2+}-containing solution and subsequent rinsing and immersion in a Cu^{2+}-free solution [37]. Here we report a study, using cyclic voltammetry (CV) and in-situ scanning tunneling microscopy (STM), of the electroreduction of preadsorbed Cu^{2+} on cyanide-modified Pt(111) electrodes, in a process analogous to that developed by Kolb and co-workers [26-32].

Experimental

The working electrodes used for CV were bead-type platinum single crystals (2 mm in diameter) prepared according to the method developed by Clavilier et al. [38], oriented and polished parallel to the (111) plane (miscut < 0.05º). The Pt(111) electrode used for STM experiments was a single-crystal disc (10 mm in diameter) purchased from MaTeck (Jülich, Germany). Before each experiment, the electrodes were annealed in the flame of a Bunsen burner and cooled in a H_2-N_2 atmosphere.

Cyanide-modified Pt(111) electrodes were prepared by immersion of a clean and well-ordered Pt(111) surface in a 0.1 M KCN (Merck, p.a.) solution for approximately 3 minutes, after which the electrode was rinsed with ultrapure water. Preadsorption of Cu^{2+} was achieved by immersing the cyanide-

modified Pt(111) electrode in either 0.1 M H_2SO_4 + 1 mM $CuSO_4$ (for subsequent experiments in 0.1 M H_2SO_4) or 0.1 M $HClO_4$ + 1 mM $Cu(ClO_4)_2$ (for subsequent experiments in 0.1 M $HClO_4$) for approximately 3 minutes, after which the electrode was rinsed with ultrapure water and transferred to the electrochemical cell containing the cyanide- and Cu^{2+}-free electrolyte (either 0.1 M H_2SO_4 or 0.1 M $HClO_4$).

The auxiliary electrodes were platinum wires. Either a reversible hydrogen electrode (RHE, used in CV experiments), or a platinum wire (STM experiments) were used as reference and quasi-reference electrodes, respectively. All the potentials in the text are referred to the RHE.

A PicoLE Molecular Imaging STM with a PicoScan 2100 Controller was used. Experiments were performed with tungsten tips, etched from a polycrystalline wire in 2 M NaOH and coated with an electrophoretic paint in order to reduce the faradaic current at the tip/electrolyte interface. All images were recorded in the constant-current mode.

Results

Cyclic Voltammetry

Figure 1(A) shows the CVs, in Cu^{2+}-free 0.1 M H_2SO_4 (red line) and 0.1 M $HClO_4$ (blue line) solutions, of a cyanide-modified Pt(111) electrode onto which Cu^{2+} had been preadsorbed, either by immersion in 0.1 M H_2SO_4 + 1 mM $CuSO_4$ (red line), or in 0.1 M $HClO_4$ + 1 mM $Cu(ClO_4)_2$ (blue line). The CV of a cyanide-modified Pt(111) electrode in 0.1 M H_2SO_4 (black line) is also shown for comparison. (Please note that the CVs of cyanide-modified Pt(111) in H_2SO_4 and $HClO_4$ show no significant differences at all [39,40].)

The CV in 0.1 M H_2SO_4 when Cu^{2+} had been preadsorbed on cyanide-modified Pt(111), but is not present in the solution, is very different from that obtained in copper-containing solutions (see red line in Figure 2 of ref. [35]). In 0.1 M H_2SO_4, a new reversible process appears at 0.38 V when Cu^{2+} has been preadsorbed, no change being observed in the CV upon repetitive cycling between 0.10 V and 1.00 V. The absence of any changes upon repetitive cycling, together with the absence of the peaks typically associated to the underpotential deposition (upd) of Cu on Pt(111), strongly suggests that the $(2\sqrt{3}$ x $2\sqrt{3})$R30º structure of the cyanide adlayer remains unaltered, and no cyanide stripping occurs as a consequence of the new process emerging at 0.38 V. Interestingly, the reversible process around 0.38 V is absent from the CV of a cyanide-modified Pt(111), onto which Cu^{2+} had been preadsorbed, in 0.1 M $HClO_4$.

We have recently shown that the hydrogen adsorption region (E < 0.6 V, black line in Figure 1(A)) of the CV of a cyanide-modified Pt(111) electrode corresponds to a proton-coupled electron transfer (PCET) to the nitrogen atom of CN_{ad} to yield CNH_{ad} [41]. In the presence of alkali-metal cations, the latter compete with H^+ for the same adsorption sites (namely, the nitrogen atom of CN_{ad}), and have to be removed from these sites before the PCET can take place, which provokes a negative shift of the hydrogen-adsorption region [36,42]. The hydrogen adsorption region of the CV in 0.1 M $HClO_4$ in Figure 1(A) is remarkably similar to that of a cyanide-modified Pt(111) electrode in 0.1 M H_2SO_4 or $HClO_4$ containing 0.05 M K^+ (see Figure S5 of ref. [36]), suggesting that the interaction of Cu^{2+} irreversibly preadsorbed on cyanide-modified Pt(111) with CN_{ad} is similar to that of K^+ at a 0.05 M concentration. In addition, the similitude between the CVs in $HClO_4$ and H_2SO_4 in Figure 1(A), excluding the feature at 0.38 V, suggests that the process associated to the latter peak does not provoke any change on the structure of the cyanide adlayer.

In the presence of preadsorbed Cu^{2+}, the double-layer corrected charge in the potential region between 0.64 and 0.10 V amounts to 98 μC cm^{-2} in 0.1 M $HClO_4$, and to 101 μC cm^{-2} in 0.1 M H_2SO_4 (in both cases, these are the average of the charges in the cathodic and anodic sweeps). These values are larger than the charge obtained for cyanide-modified Pt(111) electrodes in 0.1 M H_2SO_4 in the absence of preadsorbed Cu^{2+} (ca. 80 μC cm^{-2}, similar to the value obtained in previous work [43], even when an alkaline-metal cation is present in the solution [36]). This might be an indication that the interaction between Cu^{2+} and CN_{ad} is not purely electrostatic, and involves some degree of covalency, as also suggested by the fact that Cu^{2+} adsorption on cyanide-modified Pt(111) is irreversible (on the contrary, adsorption of alkaline-metal cations on cyanide-modified Pt(111) electrodes is only possible in the presence of the cation in the bulk of the solution [36]). A weak covalent bond between Cu^{2+} and CN_{ad} would affect the dipole moment of the latter species, and through it, the capacitance of the electrical double layer.

If we attribute the 3 μC cm^{-2} increase in the double-layer corrected charge in the potential region between 0.64 and 0.10 V measured in 0.1 MH_2SO_4, as compared to 0.1 M $HClO_4$, to the reduction of Cu^{2+} to Cu, this would correspond to the deposition of ca. 0.6% of a monolayer of Cu (referred to the atomic density of the Pt(111) substrate, i.e., 480 μC cm^{-2} per monolayer if 2 electrons are transferred). The charge under the peak at 0.38 V amounts to 5.5 μC cm^{-2} (average of the charges under the cathodic and anodic peaks, 4 and 7 μC cm^{-2}, respectively; integrated using a horizontal line at the base of the peak as baseline), which would correspond to the deposition of a slightly higher amount of Cu, 1.1% of a monolayer. However, these numbers have to be taken with care, because Cu deposition and sulfate adsorption occur concomitantly, as demonstrated by the fact that the peak at 0.38 V is only observed in sulfuric acid solutions. Sulfate adsorption and Cu electrodeposition involve the flow of charges of opposite sign, and the Cu coverage, as determined from the integrated charges in the CV, will always be underestimated.

Figure 1(B) shows a plot of the current density of the peak at 0.38 V vs. the scan rate. The linear dependence confirms that the process at 0.38 V involves a surface-confined species.

In-situ STM

The changes in the structure and morphology of the surface of a cyanide-modified Pt(111) electrode associated to the peak at 0.38 V observed in 0.1 M H_2SO_4 solutions were studied using in-situ STM. In spite of the absence of Cu^{2+} ions in the solution, the honeycomb structure typical of cations non-covalently attached on the surface of a cyanide-modified Pt(111) electrode [36] can still be observed when Cu^{2+} has been preadsorbed (Figure 2), although with more defects than in copper-containing solutions [35], which confirms that the immersion of the electrode in a Cu^{2+}-containing solution in the preadsorption step resulted in the irreversible adsorption of Cu^{2+}.

Figure 3 shows a series of images of the same 50 x 50 nm^2 area of the electrode surface obtained in 0.1 M H_2SO_4 when the potential is sequentially decreased below 0.40 V. At 0.40 V (Figure 3A), well within the hydrogen adsorption region but just more positive than the peak at 0.38 V, STM images are frizzy, a typical indication of a high surface mobility. Small protrusions ca. 0.5 nm in diameter and less than 0.1 nm in height, with some tendency to arrange themselves hexagonally, are also typically observed in this potential region. No clear change is observed when the potential is stepped from 0.40 to 0.35 V. However, when the potential is further decreased to 0.30 V (Figure 3B), some bigger features appear on the surface. Some islands form, with some preference to nucleate at monoatomic steps (see top right corner in Figure 3B). At 0.30 V, these islands continue to grow (Figure 3C), probably by diffusion and coalescence of smaller islands into bigger ones (Ostwald ripening). Although some preference for the nucleation of islands at steps is appreciable, interestingly these islands tend to grow

into the terrace, rather than parallel to the steps. The growth of the islands at $E \leq 0.30$ becomes evident by comparing the island within the white circle in Figures 3D and E. These islands were not observed in perchloric acid solutions, in agreement with the absence of the peak in the corresponding CVs. Figure 3(F) shows the height profile along the straight blue line in Figure 3(E). The total height of the monoatomic step separating the two adjacent terraces (ca. 0.23 nm) coincides with that expected with a monoatomic step on Pt(111). The apparent height of ca. 0.15 nm of the Cu nanoislands is clearly lower (which can also be inferred by the lower contrast in the STM images), but care must be taken not to overinterpret this number, because it results from a convolution of topographic and electronic effects (actual height of the island plus changes in the local tunneling barrier).

The honeycomb structure is recovered when the potential is stepped back, as illustrated in Figure 4. As indicated by the white arrow in Figures 4A and B, the honeycomb structure also reappears in the areas where islands had been formed at $E < 0.38$ V, confirming that copper deposition did not result in stripping of the cyanide adlayer.

As shown in the bottom half of Figure 5A, if, instead of gradually making the potential more negative, we step directly from 0.55 to 0.25 V, islands with a narrower size distribution appear on the surface. Again, step decoration is evident, and the honeycomb structure reappears on the surface when the potential is stepped back to 0.55 V, with no evident sign of stripping of the cyanide adlayer underneath the islands (Figure 5B).

The islands observed in Figures 3 to 5 cover approximately 16% of the imaged area, which agrees well with the 16.7% coverage expected if all the cations in the honeycomb structure (1/6 ML) are reduced to their metallic state. This coverage is, however, much larger than that deduced from the charge in the corresponding CV (between 0.6 and 1.1% of a monolayer, see above). We attribute this difference to the flow of current of opposite directions due to the concomitant electroreduction of Cu^{2+} and electroadsorption of sulfate.

The structure of the islands formed at $E < 0.40$ V could be imaged with atomic resolution (Figure 4C and inset in Figure 5A). Although the domains imaged are too small to determine the lattice constants with adequate accuracy, the distance between tunneling maxima is too large to correspond to the interatomic distance between Cu atoms. Furthermore, two rotational domains, and up to three rotational domains, can be clearly observed in the inset in Figure 5A and in Figure 4C, respectively. This is a clear indication that the periodicity is different along the two main crystallographic directions of the imaged structure.

Discussion

The change in the CV of a cyanide-modified Pt(111) electrode after the preadsorption step in Cu^{2+}-containing solutions clearly shows that Cu^{2+} ions were irreversibly adsorbed on the surface via non-covalent interactions with the nitrogen atoms of the CN_{ad} groups. The process at 0.38 V in the CVs in 0.1 M H_2SO_4 must correspond to the reduction of irreversibly adsorbed Cu^{2+} to Cu. The linear increase of the current density of this peak with increasing scan rate confirms that this is a surface-confined process, and the very small separation between the anodic and the cathodic peak potentials also indicates that the reduction of surface-confined Cu^{2+} to Cu, as well as the reoxidation of Cu to non-covalently retained Cu^{2+}, must be very fast processes.

In situ STM in 0.1 M H_2SO_4 clearly shows that two dimensional islands, easily identifiable as metallic Cu, form when the potential is made more negative than 0.38 V, confirming the conclusions reached from the CVs. Furthermore, our in-situ STM experiments also indicate that, if the potential is slowly scanned in the negative direction, or if the potential is held at $E < 0.38$ V for long periods, the islands

formed upon reduction of the surface-confined Cu^{2+} ions slowly grow by an Ostwald ripening process, in which small islands coalesce with each other, and larger islands grow at the expense of smaller ones (a process that cannot be observed with cyclic voltammetry, since it involves no charge transfer).

An important question that deserves further discussion is whether these islands correspond to a Cu adlayer on the Pt(111) substrate, or, rather, are the result of the metallization of the cyanide adlayer, yielding a Pt-CN_{ad}-Cu sandwich configuration. Although the tendency to decorate monoatomic steps separating atomically flat terraces might suggest a direct deposition of Cu on the Pt substrate, this should result in a partial stripping of the cyanide adlayer, no sign of which is visible either in the CVs or in the STM images. In particular, the latter clearly show that the cyanide adlayer maintains its integrity even directly underneath an area where a Cu island had been formed and subsequently oxidized. Accordingly, we attribute the peak at 0.38 V in the CVs of cyanide-modified Pt(111) in 0.1 M H_2SO_4, and the bidimensional islands observed with in-situ STM, to the metallization of the cyanide adlayer with Cu in a sandwich configuration. Alternatively, deposition of Cu on the Pt(111) substrate might result in a compression of the cyanide adlayer, which would relax back to the unperturbed structure upon Cu dissolution. Although we cannot discard this possibility completely, it appears less likely to us for the following reasons:

i) As we have shown recently [41], the adsorption energy of cyanide on Pt(111) increases linearly with increasing coverage, from approximately -3.25 eV at θ_{CN} = 0.25 (that of the ($2\sqrt{3}$ x $2\sqrt{3}$)R30º structure of the cyanide-modifed Pt(111) surface) to ca. -2.30 eV at θ_{CN} = 1. A compression of the cyanide adlayer by 16% (the fraction of the surface covered by the Cu islands, as revealed by STM, which would increase θ_{CN} from 0.5 to 0.58) would imply a decrease of the adsorption energy of cyanide of approximately 0.2 eV, which would impose an activation barrier for the deposition process which is not compatible with the very reversible nature of the spikes at 0.38 V observed in the corresponding CV.

ii) Even in the absence of cyanide on the surface, Cu-upd on Pt(111) is a process much slower than that observed on cyanide-modified Pt(111), with a clear separation between the peak potentials of the anodic and cathodic upd peaks even at 1 mV s^{-1} [35].

iii) In our experience, the shape of the hydrogen adsorption region in the CV of a cyanide-modified Pt(111) electrode is very sensitive to the quality (i.e., coverage and structure) of the cyanide adlayer. If the cyanide adlayer is compressed upon Cu deposition, we would expect a clear change in the shape of the CV. On the contrary, the shapes of the CVs in 0.1 M $HClO_4$ (where no Cu deposition takes place) and in 0.1 M H_2SO_4 at potentials negative of the deposition peak are nearly identical.

The absence of the peak at 0.38 V in perchloric acid solutions suggests that metallization of the cyanide adlayer is only made energetically favorable thanks to the specific adsorption of sulfate on the Cu islands. This case is similar to that of Cu-upd on Au(111) in sulfuric acid solutions, which has been recently shown to be possible thanks to the stabilization of the Cu(1 x 1) pseudomorphic layer on Au(111) by adsorbed sulfate [44], even though the binding energy of a Cu(1 x 1) monolayer on Au(111) is smaller than the bulk binding energy of Cu [45-48]. The observation in atomically resolved in-situ STM images of the Cu nanoislands on cyanide-modified Pt(111) electrodes of up to three rotational domains, as expected for the ($\sqrt{3} \times \sqrt{7}$)R30º usually observed on the (111) faces of *fcc* metals [49-58] provides additional support to this conclusion. Interestingly, in perchloric acid solutions reduction of Cu^{2+} irreversibly adsorbed on cyanide-modified Pt(111) electrodes to Cu is not possible even at potential as negative as 0.1 V, well below the corresponding standard equilibrium potential.

Conclusions

The results reported here strongly suggest that Cu^{2+} ions irreversibly retained on the surface of a cyanide-modified Pt(111) electrode can be reduced to their metallic state in sulfuric acid solutions, resulting in the metallization of the cyanide adlayer with bidimensional Cu nanoislands. This reduction is impossible in perchloric acid solutions, suggesting that it is the presence of a specifically adsorbing anion like sulfate what makes a copper island deposited on the cyanide adlayer stable. The Cu nanoislands are mobile and can diffuse over the electrode surface, bigger islands slowly growing at the expense of smaller ones via an Ostwald ripening mechanism. Future work will focus on: (i) combining adsorbates with functional groups that enable them to retain metal cations on the electrode surface irreversibly, like mercaptopyridine [25-30,32-34], diazobenzene [31], or cyanide ([35], this work), with adsorbates that can act as a barrier for the diffusion of ions and small groups of metal atoms, with the aim of achieving an ordered deposit of naonislands of similar sizes; (ii) studying, using current-sensing AFM, the conductance of the substrate-molecule-nanoisland sandwich; and (iii) determining the electronic structure and, eventually, the magnetic properties of the naoislands using optical methods (like, e.g, potential-modulated reflectance spectroscopy and surface magneto-optic Kerr effect).

Acknowledgement

The support of the University of Aberdeen is gratefully acknowledged. CW acknowledges a summer studentship from the Carnegie Trust for the Universities of Scotland.

References

1. Reed MA, Zhou C, Muller CJ, Burgin TP, Tour JM (1997) Conductance of a Molecular Junction. Science 278:252-254
2. Fink H-W, Schonenberger C (1999) Electrical conduction through DNA molecules. Nature 398:407-410
3. Gimzewski JK, Joachim C (1999) Nanoscale Science of Single Molecules Using Local Probes. Science 283:1683-1688
4. Gittins DI, Bethell D, Schiffrin DJ, Nichols RJ (2000) A nanometre-scale electronic switch consisting of a metal cluster and redox-addressable groups. Nature 408:67-69
5. Porath D, Bezryadin A, de Vries S, Dekker C (2000) Direct measurement of electrical transport through DNA molecules. Nature 403:635-638
6. Cui XD, Primak A, Zarate X, Tomfohr J, Sankey OF, Moore AL, Moore TA, Gust D, Harris G, Lindsay SM (2001) Reproducible Measurement of Single-Molecule Conductivity. Science 294:571-574
7. Liang W, Shores MP, Bockrath M, Long JR, Park H (2002) Kondo resonance in a single-molecule transistor. Nature 417:725-729
8. Moresco F, Gross L, Alemani M, Rieder K-H, Tang H, Gourdon A, Joachim C (2003) Probing the Different Stages in Contacting a Single Molecular Wire. Phys Rev Lett 91:036601
9. Xu B, Tao NJ (2003) Measurement of Single-Molecule Resistance by Repeated Formation of Molecular Junctions. Science 301:1221-1223
10. Dadosh T, Gordin Y, Krahne R, Khivrich I, Mahalu D, Frydman V, Sperling J, Yacoby A, Bar-Joseph I (2005) Measurement of the conductance of single conjugated molecules. Nature 436:677-680
11. Guo S, Artés JM, Díez-Pérez I (2013) Electrochemically-gated single-molecule electrical devices. Electrochim Acta 110:741-753
12. Chen J, Reed MA, Rawlett AM, Tour JM (1999) Large On-Off Ratios and Negative Differential Resistance in a Molecular Electronic Device. Science 286:1550-1552
13. Lörtscher E (2013) Wiring molecules into circuits. Nat Nanotech 8:381-384

14. Jung DR, Czanderna AW (1994) Chemical and physical interactions at metal/self-assembled organic monolayer interfaces. Crit Rev Solid State Mater Sci 19:1-54
15. Smith EL, Alves CA, Anderegg JW, Porter MD, Siperko LM (1992) Deposition of metal overlayers at end-group-functionalized thiolate monolayers adsorbed at gold. 1. Surface and interfacial chemical characterization of deposited copper overlayers at carboxylic acid-terminated structures. Langmuir 8:2707-2714
16. Sun L, Crooks RM (1991) Imaging of Defects Contained within n-Alkylthiol Monolayers by Combination of Underpotential Deposition and Scanning Tunneling Microscopy: Kinetics of Self-Assembly. J Electrochem Soc 138:L23-L25
17. Gilbert SE, Cavalleri O, Kern K (1996) Electrodeposition of Cu Nanoparticles on Decanethiol-Covered Au(111) Surfaces: An in Situ STM Investigation. J Phys Chem 100:12123-12130
18. Nishizawa M, Sunagawa T, Yoneyama H (1997) Underpotential Deposition of Copper on Gold Electrodes through Self-Assembled Monolayers of Propanethiol. Langmuir 13:5215-5217
19. Zamborini FP, Campbell JK, Crooks RM (1998) Spectroscopic, Voltammetric, and Electrochemical Scanning Tunneling Microscopic Study of Underpotentially Deposited Cu Corrosion and Passivation with Self-Assembled Organomercaptan Monolayers. Langmuir 14:640-647
20. Cavalleri O, Bittner AM, Kind H, Kern K, Greber T (1999) Copper Electrodeposition on Alkanethiolate Covered Gold Electrodes. Z Phys Chem 208:107-136
21. Hagenström H, Schneeweiss MA, Kolb DM (1999) Modification of a Au(111) Electrode with Ethanethiol. 2. Copper Electrodeposition. Langmuir 15:7802-7809
22. Hagenström H, Schneeweiss MA, Kolb DM (1999) Copper underpotential deposition on ethanethiol-modified Au(111) electrodes: kinetic effects. Electrochim Acta 45:1141-1145
23. Oyamatsu D, Kuwabata S, Yoneyama H (1999) Underpotential deposition behavior of metals onto gold electrodes coated with self-assembled monolayers of alkanethiols. J Electroanal Chem 473:59-67
24. Schneeweiss MA, Hagenström H, Esplandiu MJ, Kolb DM (1999) Electrolytic metal deposition onto chemically modified electrodes. Appl Phys A 69:537-551
25. Baunach T, Kolb DM (2002) The electrochemical characterisation of benzyl mercaptan-modified Au(111): Structure and copper deposition. Anal Bioanal Chem 373:743-748
26. Baunach T, Ivanova V, Kolb DM, Boyen HG, Ziemann P, Büttner M, Oelhafen P (2004) A New Approach to the Electrochemical Metallization of Organic Monolayers: Palladium Deposition onto a 4,4'-Dithiodipyridine Self-Assembled Monolayer. Adv Mater 16:2024-2028
27. Ivanova V, Baunach T, Kolb DM (2005) Metal deposition onto a thiol-covered gold surface: A new approach. Electrochim Acta 50:4283-4288
28. Manolova M, Ivanova V, Kolb DM, Boyen HG, Ziemann P, Büttner M, Romanyuk A, Oelhafen P (2005) Metal deposition onto thiol-covered gold: Platinum on a 4-mercaptopyridine SAM. Surf Sci 590:146-153
29. Boyen H-G, Ziemann P, Wiedwald U, Ivanova V, Kolb DM, Sakong S, Gross A, Romanyuk A, Buttner M, Oelhafen P (2006) Local density of states effects at the metal-molecule interfaces in a molecular device. Nat Mater 5:394-399
30. Manolova M, Kayser M, Kolb DM, Boyen HG, Ziemann P, Mayer D, Wirth A (2007) Rhodium deposition onto a 4-mercaptopyridine SAM on Au(111). Electrochim Acta 52:2740-2745
31. Eberle F, Metzler M, Kolb DM, Saitner M, Wagner P, Boyen H-G (2010) Metallization of Ultra-Thin, Non-Thiol SAMs with Flat-Lying Molecular Units: Pd on 1, 4-Dicyanobenzene. ChemPhysChem 11:2951-2956
32. Eberle F, Saitner M, Boyen H-G, Kucera J, Gross A, Romanyuk A, Oelhafen P, D'Olieslaeger M, Manolova M, Kolb DM (2010) A Molecular Double Decker: Extending the Limits of Current Metal–Molecule Hybrid Structures. Angew Chem Int Ed 49:341-345
33. Silien C, Lahaye D, Caffio M, Schaub R, Champness NR, Buck M (2011) Electrodeposition of Palladium onto a Pyridine-Terminated Self-Assembled Monolayer. Langmuir 27:2567-2574

34. Shekhah O, Busse C, Bashir A, Turcu F, Yin X, Cyganik P, Birkner A, Schuhmann W, Woll C (2006) Electrochemically deposited Pd islands on an organic surface: the presence of Coulomb blockade in STM I(V) curves at room temperature. Phys Chem Chem Phys 8:3375-3378
35. Escudero M, Marco JF, Cuesta A (2009) Surface Decoration at the Atomic Scale Using a Molecular Pattern: Copper Adsorption on Cyanide-Modified Pt(111) Electrodes. J Phys Chem C 113:12340-12344
36. Escudero-Escribano M, Zoloff Michoff ME, Leiva EPM, Marković NM, Gutiérrez C, Cuesta Á (2011) Quantitative Study of Non-Covalent Interactions at the Electrode–Electrolyte Interface Using Cyanide-Modified Pt(111) Electrodes. ChemPhysChem 12:2230-2234
37. Escudero Escribano M (2011) Electrocatalysis and surface nanostructuring : atomic ensemble effects and non-covalent interactions. Universidad Autónoma de Madrid, http://hdl.handle.net/10261/42378
38. Clavilier J, Faure R, Guinet G, Durand R (1979) Preparation of monocrystalline Pt microelectrodes and electrochemical study of the plane surfaces cut in the direction of the {111} and {110} planes. J Electroanal Chem 107:205-209
39. Huerta F, Morallón E, Quijada C, Vázquez JL, Aldaz A (1998) Spectroelectrochemical study on CN− adsorbed at Pt(111) in sulphuric and perchloric media. Electrochim Acta 44:943-948
40. Strmcnik D, Escudero-Escribano M, Kodama K, Stamenkovic VR, Cuesta A, Marković NM (2010) Enhanced electrocatalysis of the oxygen reduction reaction based on patterning of platinum surfaces with cyanide. Nat Chem 2:880-885
41. Escudero-Escribano M, Soldano GJ, Quaino P, Zoloff Michoff ME, Leiva EPM, Schmickler W, Cuesta Á (2012) Cyanide-modified Pt(111): Structure, stability and hydrogen adsorption. Electrochim Acta 82:524-533
42. Wildi C, Cabello G, Zoloff Michoff ME, Vélez P, Leiva EPM, Calvente JJ, Andreu R, Cuesta A (2015) Super-Nernstian Shifts of Interfacial Proton-Coupled Electron Transfers: Origin and Effect of Non-Covalent Interactions. J Phys Chem C, DOI: 10.1021/acs.jpcc.5b04560
43. Morales-Moreno I, Cuesta A, Gutiérrez C (2003) Accurate determination of the CO coverage at saturation on a cyanide-modified Pt(111) electrode in cyanide-free 0.5 M H2SO4. J Electroanal Chem 560:135-141
44. Vélez P, Cuesta A, Leiva EPM, Macagno VA (2012) The underpotential deposition that should not be: Cu(1 x 1) on Au(111). Electrochem Commun 25:54-57
45. Sánchez C, Leiva E (1998) Underpotential versus overpotential deposition: a first-principles calculation. J Electroanal Chem 458:183-189
46. Sánchez C, Leiva EPM (1999) Cu underpotential deposition on Au(111) and Au(100). Can this be explained in terms of the energetics of the Cu/Au system? Electrochim Acta 45:691-697
47. Sanchez CG, Leiva EPM, Kohanoff J (2001) Relevance of Heterometallic Binding Energy for Metal Underpotential Deposition. Langmuir 17:2219-2227
48. Greeley J (2010) Structural effects on trends in the deposition and dissolution of metal-supported metal adstructures. Electrochim Acta 55:5545-5550
49. Magnussen OM, Hagebock J, Hotlos J, Behm RJ (1992) In situ scanning tunnelling microscopy observations of a disorder-order phase transition in hydrogensulfate adlayers on Au(111). Faraday Discussions 94:329-338
50. Edens GJ, Gao X, Weaver MJ (1994) The adsorption of sulfate on gold(111) in acidic aqueous media: adlayer structural inferences from infrared spectroscopy and scanning tunneling microscope. J Electroanal Chem 375:357-366
51. Funtikov AM, Linke U, Stimming U, Vogel R (1995) An in-situ STM study of anion adsorption on Pt(111) from sulfuric acid solutions. Surf Sci 324:L343-L348
52. Wan L-J, Yau S-L, Itaya K (1995) Atomic Structure of Adsorbed Sulfate on Rh(111) in Sulfuric Acid Solution. J Phys Chem 99:9507-9513

53. Funtikov AM, Stimming U, Vogel R (1997) Anion adsorption from sulfuric acid solutions on Pt(111) single crystal electrodes. J Electroanal Chem 428:147-153
54. Li W-H, Nichols RJ (1998) An in situ STM study of sulphate adsorption on copper(111) in acidic aqueous electrolytes. J Electroanal Chem 456:153-160
55. Wilms M, Broekmann P, Kruft M, Park Z, Stuhlmann C, Wandelt K (1998) STM investigation of specific anion adsorption on Cu(111) in sulfuric acid electrolyte. Surf Sci 402–404:83-86
56. Wan L-J, Hara M, Inukai J, Itaya K (1999) In Situ Scanning Tunneling Microscopy of Well-Defined Ir(111) Surface: High-Resolution Imaging of Adsorbed Sulfate. J Phys Chem B 103:6978-6983
57. Wan L-J, Suzuki T, Sashikata K, Okada J, Inukai J, Itaya K (2000) In situ scanning tunneling microscopy of adsorbed sulfate on well-defined Pd(111) in sulfuric acid solution. J Electroanal Chem 484:189-193
58. Cuesta A, Kleinert M, Kolb DM (2000) The adsorption of sulfate and phosphate on Au(111) and Au(100) electrodes: an in situ STM study. Phys Chem Chem Phys 2:5684-5690

Figure Captions

Figure 1. (A) Cyclic voltammograms at 50 mV s^{-1} of a cyanide-modified Pt(111) electrode in 0.1 M H_2SO_4 (black line), in 0.1 M H_2SO_4 after preadsorption of Cu^{2+} by immersion in a 0.1 M H_2SO_4 + 1 mM $CuSO_4$ solution (red line), and in 0.1 M $HClO_4$ after preadsorption of Cu^{2+} by immersion in a 0.1 M $HClO_4$ + 1 mM Cu_2SO_4 solution (blue line). (B) Plot of the peak current density vs. the scan rate of the peak observed in 0.1 M H_2SO_4 at 0.38 V after preadsorption of Cu^{2+}.

Figure 2. 50 x 50 nm^2 STM image at 0.55 V in Cu^{2+}-free 0.1 M H_2SO_4 of a cyanide-modified Pt(111) electrode onto which Cu^{2+} had been preadsorbed by immersion in a 0.1 M H_2SO_4 + 1 mM $CuSO_4$ solution; U_T = 0.25 V (tip negative); I_T = 2 nA.

Figure 3. Sequence of images in 0.1 M H_2SO_4 of the same 50 x 50 nm^2 area of a cyanide-modified Pt(111) electrode onto which Cu^{2+} had been preadsorbed, recorded as the potential was sequentially decreased from 0.40 to 0.25 V. (A) 0.40 V, U_T = 0.10 V (tip negative); (B) the potential was stepped from 0.35 (U_T = 0.15 V, tip negative) to 0.30 V (U_T = 0.10 V, tip negative) at the point marked with an arrow (scan direction from bottom to top); (C) 0.30 V, U_T = 0.10 V (tip negative); (D) 0.25 V, U_T = 0.10 V (tip negative); (E) 0.25 V, U_T = 0.10 V (tip negative). I_T = 2 nA in all the images. The white circles in (D) and (E) identify the same island, and serve to illustrate its growth at 0.25 V; (F) Height profile along the blue straight line in (E).

Figure 4. (A) STM image (50 x50 nm^2) in 0.1 M H_2SO_4 of the same area of a cyanide-modified Pt(111) electrode shown in Figure 4, at 0.25 V. (B) The same area, showing the recovery of the honeycomb structure when the potential is stepped back to 0.55 V (the potential was changed at half image; scan direction from bottom to top). The white arrow in B marks the location where the island marked with the white arrow in A had formed. (C) Zoom (20 x 20 nm^2) into the area within the square in A, showing the structure of the island with atomic resolution.

Figure 5. (A) STM image (100 x 100 nm^2) in 0.1 M H_2SO_4 of a cyanide-modified Pt(111) electrode onto which Cu^{2+} had been preadsorbed after a potential step from 0.55 to 0.25 V. At half image, the potential was stepped back to 0.55 V (scan direction from bottom to top). The inset (10 x 15 nm^2) shows the structure of island in the white circle with atomic resolution. (B) Zoom (20 x 10 nm^2) into the area within the white rectangle in (A). Only half of the island marked with a white arrow had been imaged when the potential was stepped back to 0.55 V. As can be seen, after the potential step to 0.55 V, the honeycomb structure reappears intact in the area where the remaining half of the island must have been at 0.25 V.

Figure 1
Click here to download Figure: Figura 1.jpg

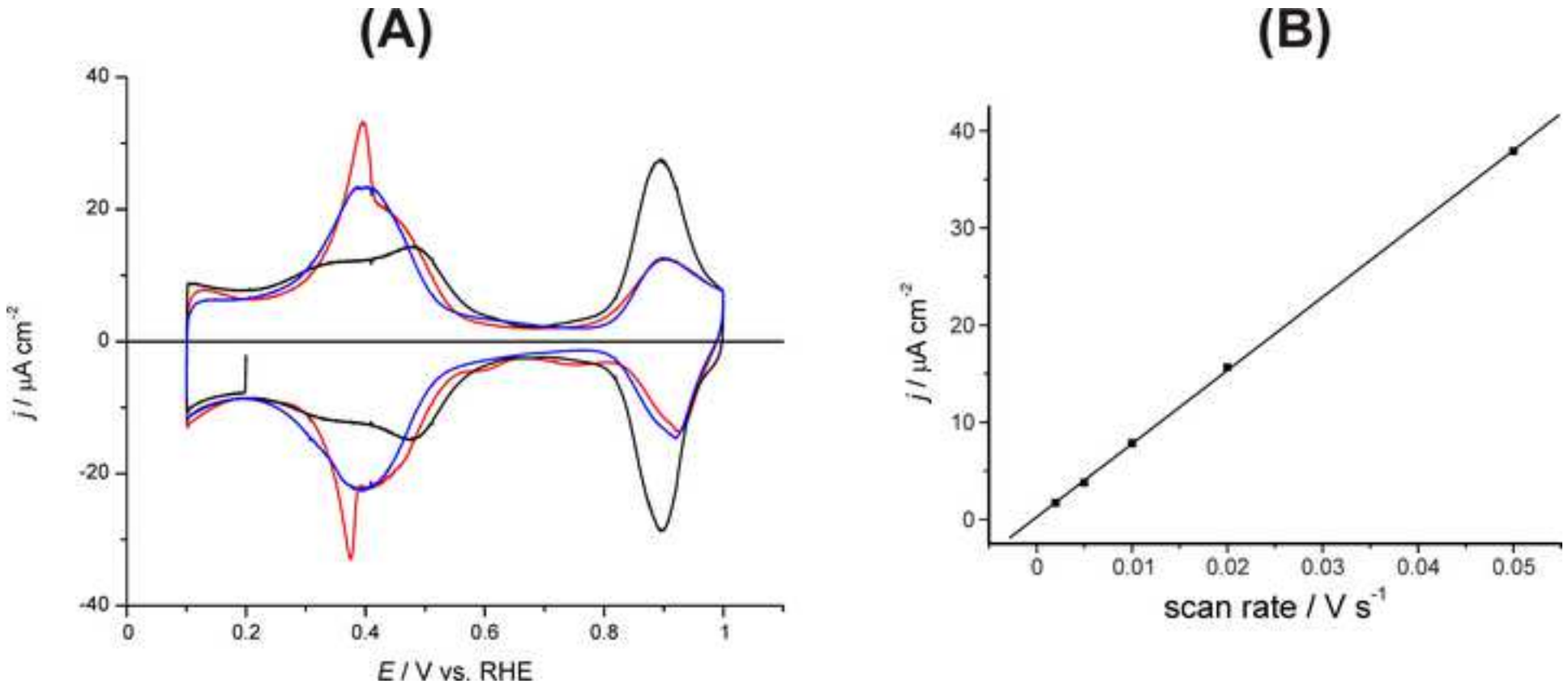

Figure 2
Click here to download Figure: Figura 2.jpg

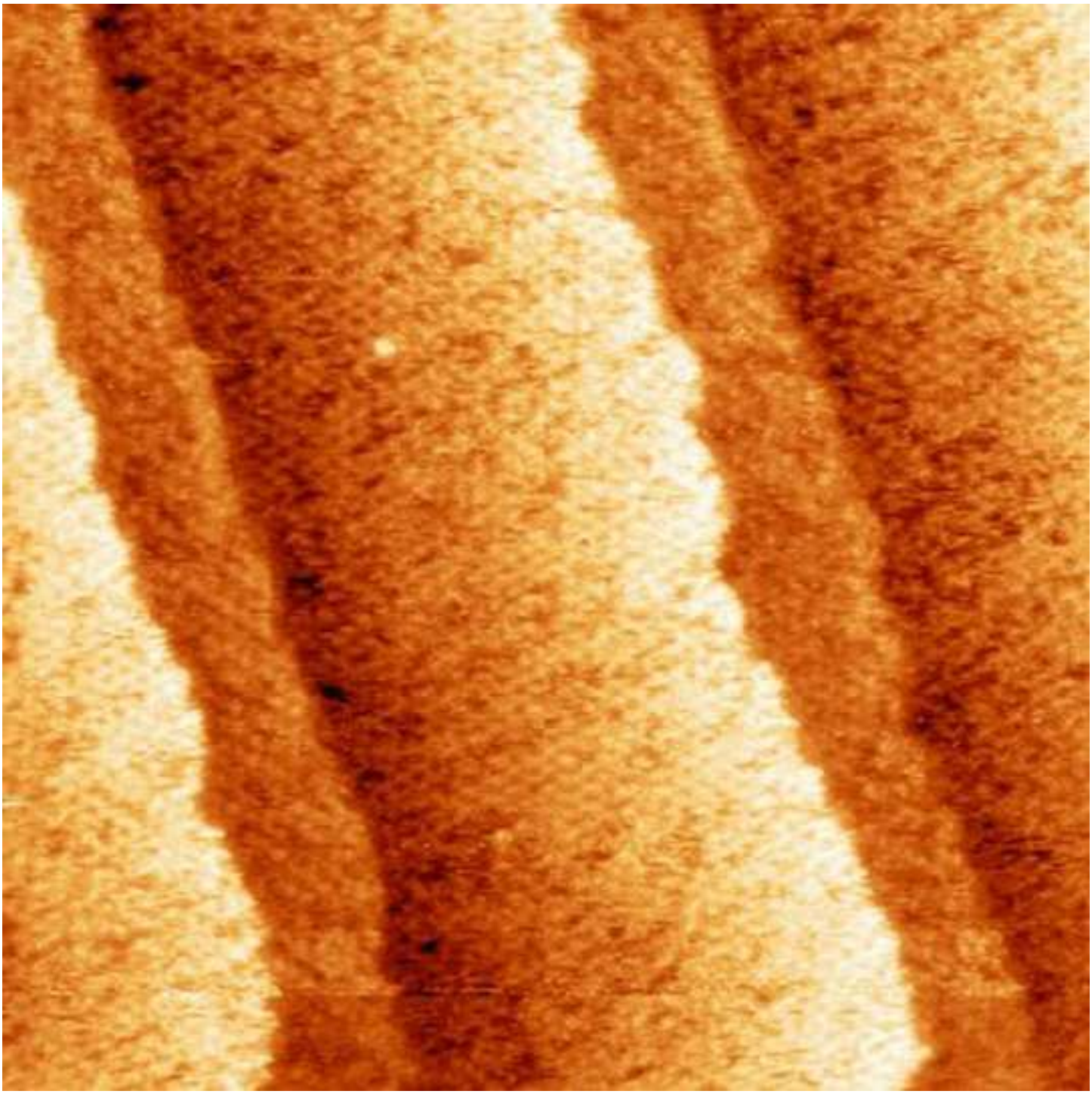

Figure 3
Click here to download Figure: Figura 3, revised.jpg

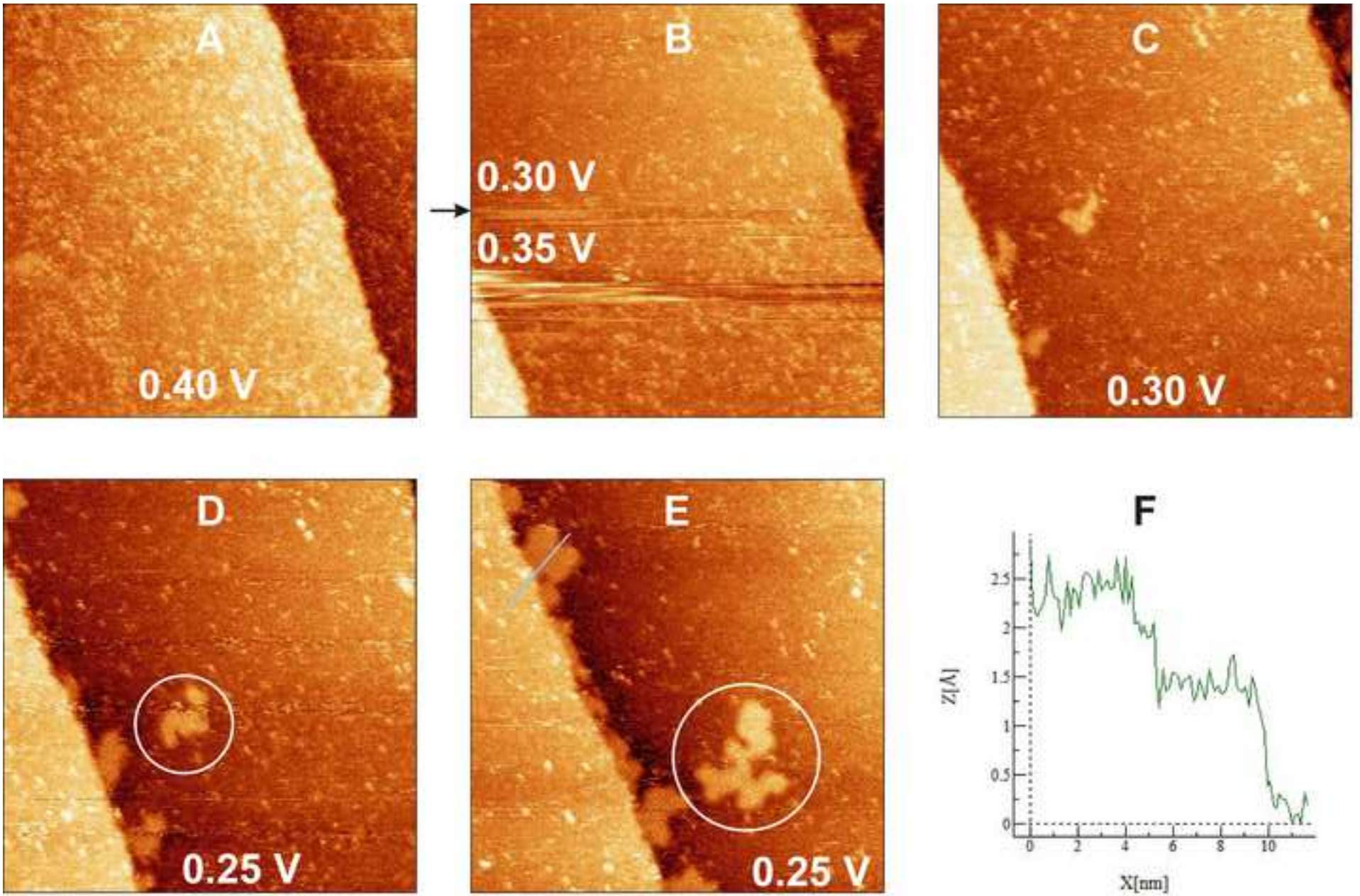

Figure 4
Click here to download Figure: Figura 4.jpg

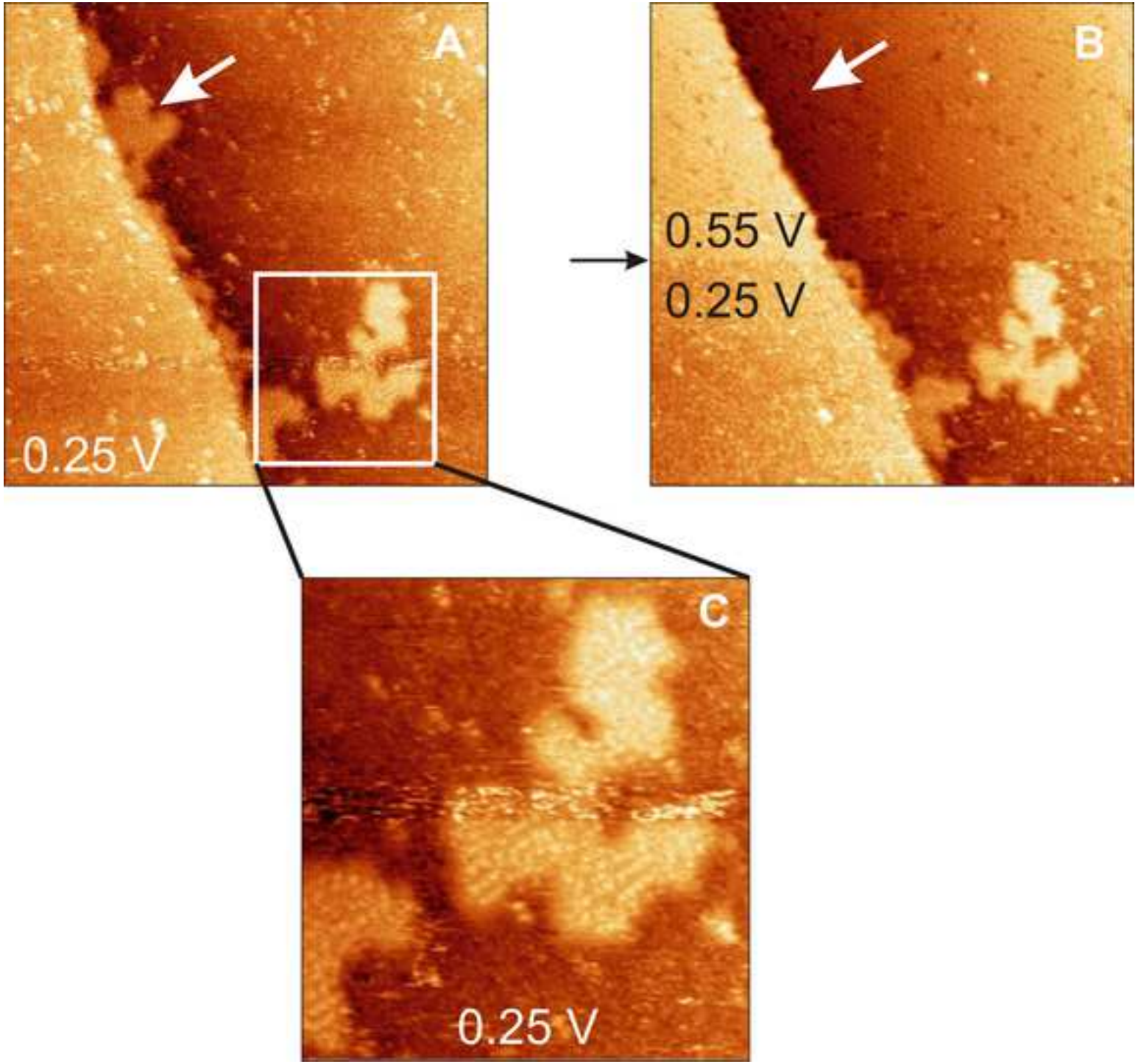

Figure 5
Click here to download Figure: Figura 5.jpg